Autoresonant beat-wave generation

R. R. Lindberg,[a)] A. E. Charman, and J. S. Wurtele
University of California, Berkeley Department of Physics, Berkeley, California 94720 and Lawrence Berkeley National Laboratory Center for Beam Physics, Berkeley, California

L. Friedland
Racah Institute of Physics, The Hebrew University, Jerusalem 91904, Israel

B. A. Shadwick
Lawrence Berkeley National Laboratory LOASIS Program, Berkeley, California and Institute for Advanced Physics, Conifer, Colorado 80433

(Received 7 August 2006; accepted 18 October 2006; published online 7 December 2006)

Autoresonance offers an efficient and robust means for the ponderomotive excitation of nonlinear Langmuir waves by phase-locking of the plasma wave to the slowly chirped beat frequency of the driving lasers via adiabatic passage through resonance. This mechanism is analyzed for the case of a cold, relativistic, underdense electron plasma, and its suitability for particle acceleration is discussed. Compared to traditional approaches, this new autoresonant scheme achieves larger accelerating electric fields for given laser intensity; the plasma wave excitation is much more robust to variations in plasma density; it is largely insensitive to the precise choice of chirp rate, provided only that it is sufficiently slow; and the suitability of the resulting plasma wave for accelerator applications is, in some respects, superior. As in previous schemes, modulational instabilities of the ionic background ultimately limit the useful interaction time, but nevertheless peak electric fields approaching the wave-breaking limit seem readily attainable. The total frequency shift required is only of the order of a few percent of the laser carrier frequency, and might be implemented with relatively little additional modification to existing systems based on chirped pulse amplification techniques, or, with somewhat greater technological effort, using a CO_2 or other gas laser system.
 [DOI: 10.1063/1.2390692]

I. INTRODUCTION AND OVERVIEW

The plasma beat-wave accelerator (PBWA) was first proposed by Tajima and Dawson (TD)[1] as an alternative to the short-pulse laser wake-field accelerator, based on earlier analysis of beat-wave excitation as a mechanism for plasma heating.[2–4] Subsequently the PBWA concept has been studied extensively theoretically, numerically, and experimentally [5–14] (for a review, see Ref. 15). In the original scheme, two lasers co-propagating in an underdense plasma are detuned from each other by a frequency shift close to the electron plasma frequency, so that the modulated envelope resulting from the beating between the lasers can act ponderomotively on the plasma electrons to resonantly excite a large-amplitude, high-phase-velocity Langmuir wave suitable for particle acceleration.

For a fixed beat frequency, performance of the PBWA is constrained by what is now known as the Rosenbluth-Liu (RL) limit, after the pioneering study in Ref. 4. As the plasma wave grows, relativistic detuning effects eventually prevent further excitation of the peak longitudinal electric field E_z beyond a maximum value E_{RL}, which lies below the cold, nonrelativistic, one-dimensional (1D), wave-breaking (WB) limit E_0:[16,17]

$$E_{\mathrm{RL}} \equiv E_0\left(\frac{16}{3}\frac{\omega_p^2}{\omega_1\omega_2}\frac{|E_1||E_2|}{E_0^2}\right)^{1/3} < E_0 \equiv \frac{mc\omega_p}{e}, \qquad (1)$$

where c is the speed of light, m is the electron mass, e is the magnitude of its charge; ω_p is the electron plasma frequency, defined in Gaussian units by $\omega_p^2 \equiv 4\pi n_0 e^2/m$, where n_0 is the ambient electron number density, E_1 and E_2 are the peak electric fields of the beating drive lasers, and ω_1 and ω_2 are their respective carrier frequencies. For the plasma waves of interest here, E_0 is smaller than the cold, relativistic (or nonlinear) wave-breaking limit:[15,16] $E_0 < E_{\mathrm{WB}} = \sqrt{2(\gamma_p - 1)}E_0$, where $\gamma_p \equiv [1 - v_p^2/c^2]^{-1/2}$. Here, v_p is the phase-velocity of the excited plasma wave, approximately equal to the characteristic group velocity $\bar{v}_g$ (to be precisely defined below) of the laser beat envelope, both of which are nearly equal to c.

The detuning effect that gives rise to the limit (1) can be understood by considering the effective nonlinear plasma frequency $\omega_{p_{\mathrm{NL}}} \approx \omega_p/\sqrt{\gamma_{\mathrm{rms}}}$, where γ_{rms} is the root-mean-square relativistic factor of the electrons, including both the transverse quiver in the laser fields and the longitudinal velocity in the Langmuir wave itself. The transverse quiver velocity is roughly constant for the fixed-amplitude driving lasers typical of the PBWA, but as the longitudinal electron motion in the excited Langmuir wave becomes weakly relativistic, γ_{rms} will increase, causing $\omega_{p_{\mathrm{NL}}}$ to decrease. Because of the sensitivity of resonance phenomena, γ_{rms} need not grow much before this resonance shift severely limits the efficacy of the driving beat-wave. As this dynamical process

[a)]Electronic address: RL236@socrates.berkeley.edu

is reversible, the Langmuir wave is not actually saturated, but exhibits a slow nonlinear modulation in amplitude, periodically peaking near $E_{\rm RL}$ as energy is exchanged between the Langmuir wave and the laser fields.

Tang, Sprangle, and Sudan (TSS)[7] pointed out that one can, in principle, achieve somewhat higher amplitudes than $E_{\rm RL}$ by detuning the beat frequency to a value below ω_p, matching $\omega_{p_{\rm NL}}$ for some nontrivial plasma wave amplitude. However, for sufficiently large detunings, the high-amplitude solution cannot be reliably accessed.[18] Shvets[19] has recently proposed a complementary approach that takes advantage of the relativistic bi-stability of the Langmuir wave to excite large-amplitude waves beyond $E_{\rm RL}$. Matte *et al.*[20] suggested countering the change in the resonance using the increase in plasma density during ionization to compensate for the nonlinear increase in $\gamma_{\rm rms}$; unfortunately, field ionization is exponentially sensitive to the laser intensity, making this method difficult to realize experimentally.

As a more practical improvement to,[20] Deutsch, Meerson, and Golub (DMG)[21] suggested incorporating compensatory time dependence into the drive laser frequencies. By chirping the laser frequency downward starting from the linear resonance ω_p, one can imagine compensating for the change in the nonlinear resonance with a corresponding change in the beat frequency. DMG invoke the nonlinear dynamical phase-locking phenomenon known as autoresonance,[22,23] arguing that the dynamical system can self-adjust to maintain phase entrainment between the driven wave and the ponderomotive drive, resulting in an increase in the oscillation amplitude without external feedback. However, proposed as it was before the understanding of autoresonance had matured, especially with regard to the threshold behavior for establishing and maintaining entrainment and the importance of an initial detuning, the DMG scheme sometimes fails to produce appreciable phase-locking.

Informed by more recent results, we propose a novel variant of the chirped PBWA concept that also exploits autoresonance, but enhanced via adiabatic passage through resonance (APTR).[24,25] Rather than chirping downward from the linear resonance, we actually start with a frequency shift well above ω_p, and then slowly sweep the beat frequency through and below resonance. With this approach, the final state of the plasma wave is insensitive to the exact chirp history, and the excitation is more robust with respect to imprecise characterization of the plasma density. The chirp rate must only be sufficiently slow so as to satisfy a certain adiabatic trapping condition and thereby ensure phase-locking. Before the onset of saturation, the frequency of the excited plasma wave can be closely entrained to the instantaneous beat frequency of the drivers, while the plasma wave amplitude grows monotonically to automatically and self-consistently adjust itself to the decreasing beat frequency.

Not only is our excitation scheme more robust, so too is our method of analysis. The Lagrangian fluid formalism developed by RL and then used by DMG employs a power series expansion which is valid only for weakly relativistic motion, so that their equations of motion become increasingly untrustworthy precisely in the regime of interest, where the plasma wave amplitude grows to some appreciable fraction of E_0. Here, we instead employ a fully nonlinear, Eulerian fluid model that allows for arbitrarily relativistic electron motion below the nonlinear wave-breaking limit $E_{\rm WB}$, similar to that discussed in Refs. 15 and 26 for laser-plasma interactions, in Ref. 9 for PBWA investigations, and was first introduced in Ref. 16.

This analytical fluid model, and the various physical assumptions which go into it, are discussed in Sec. II. In order to treat the autoresonant nature of the problem more transparently, we reformulate the dynamical equations in a fully Hamiltonian form in Sec. III. In Sec. IV, we use this canonical formalism to analyze the autoresonant aspects of the beat-wave excitation, from the initial phase-locking regime through the nonlinear trapped phase to nonadiabatic saturation. In Sec. V, we discuss features of some realistic examples relevant for possible experimental investigation. Section VI includes a fluid simulation substantiating our results with a more complicated laser-plasma model, while Sec. VII summarizes our preliminary assessment of the merits and limits of our autoresonant PBWA, especially with respect to the robust nature of excitation and the utility of phase-locking for matched electron injection. We then offer brief conclusions from our initial investigation and prospects for future study in Sec. VIII.

II. FUNDAMENTAL EQUATIONS

Our study of wake excitation is based on an approximate, but convenient and widely used model. The underdense plasma is treated as a cold, collisionless, fully relativistic electron fluid moving in a stationary, neutralizing, ionic background, coupled to electromagnetic fields governed by Maxwell's equations. The cold, collisionless treatment assumes that the electron temperature is sufficiently small so that the thermal speed is negligible compared to both the transverse quiver velocity in the driving lasers and the Langmuir phase velocity $v_p \approx c$, while stationary ions is valid provided the time scale for ion motion is longer than the duration T of the lasers; i.e., $\omega_i T \lesssim 2\pi$, where $\omega_i^2 = 4\pi n_0 Z_i^2 e^2/M_i$ is the ion plasma frequency for ions of mass M_i and charge $+Z_i e$. We restrict our analysis to 1D geometry, assuming the laser waist and any other transverse variation is much larger than the Langmuir wavelength $\lambda_p \sim c/\omega_p$. In addition, we assume prescribed laser fields, neglecting any changes to the laser envelopes due to linear effects such as diffraction, or any nonlinear back-action of the plasma on the lasers such as depletion, self-modulation, or other instabilities.[27,28] This model, although simplified, nevertheless reveals the essential features of autoresonance and its potential advantages for the PBWA.

We define a scaled, or dimensionless, time $\tau \equiv \omega_p t$, co-moving position $\xi \equiv \omega_p(t - z/\bar{v}_g)$, vector potential $\boldsymbol{a} \equiv (e/mc^2)\boldsymbol{A}$, and electrostatic potential $\phi \equiv (e/mc^2)\Phi$. Now, we further make the quasi-static approximation (QSA) (see, e.g., Refs. 9 and 29), wherein we assume that the plasma response is independent of time τ in the co-moving frame, i.e., $\phi = \phi(\xi)$, and the plasma wave moves without dispersion at the fixed average group velocity $\bar{v}_g$ of the driving lasers. Thus, in the QSA, all τ derivatives in the fluid equations are neglected, and the continuity and momentum equation can be explicitly integrated and solved, yielding a single second-order differential equation for the electrostatic potential. In the high phase-velocity limit appropriate to underdense plasmas, this equation may be simplified to

$$\frac{\partial^2}{\partial \xi^2}\phi = \frac{1}{2}\left[\frac{1+a^2}{(1+\phi)^2} - 1\right]. \tag{2}$$

After solving for $\phi(\xi)$ in (2), we can determine the electric field using $(\partial/\partial\xi)\phi = \beta_p(E_z/E_0)$. While (2) remains mathematically well defined for any $\phi > -1$, it can only be physically trusted for electric fields less than E_{WB}.

In the Coulomb gauge, the vector potential is solenoidal, which in 1D implies that it is geometrically transverse, so $\boldsymbol{a} = \boldsymbol{a}_\perp(\xi,\tau)$ will be polarized perpendicular to $\hat{z}$. For two slowly chirped, nearly-plane-wave, flat-topped lasers with positive helicity, the normalized vector potential representing the beating lasers may be written as $\boldsymbol{a} = \boldsymbol{a}_1 + \boldsymbol{a}_2 = \frac{1}{2}[\hat{\boldsymbol{e}}_+ a_1 e^{i\psi_1} + \hat{\boldsymbol{e}}_+ a_2 e^{i\psi_2} + \text{c.c.}]$, where $\hat{\boldsymbol{e}}_\pm = (1/\sqrt{2})(\hat{\boldsymbol{x}} \pm i\hat{\boldsymbol{y}})$. At the leading edge of the plasma, the laser phases are given by $\psi_j(0,t) = \psi_{j_0} - \int_0^t dt'\,\omega_j(t')$, where the ψ_{j_0} depend on initial conditions, and the instantaneous carrier frequencies $\omega_j(t) \equiv \omega_j(0,t) \equiv -(d/dt)\psi_j(0,t)$ allow for slow chirping of one or both of the lasers, such that $|\omega_j^{-1}(d/dt)\omega_j| \ll \omega_p \ll \omega_j$ and $|\bar{\omega}_1 - \bar{\omega}_2| \sim \omega_p$. We define the average carrier frequencies $\bar{\omega}_j \equiv (1/T)\int_0^T dt'\,\omega_j(t')$, and the overall average carrier frequency by $\bar{\omega} = \frac{1}{2}(\bar{\omega}_1 + \bar{\omega}_2)$.

We assume that the laser frequencies $\omega_j = -(\partial/\partial t)\psi_j$ and wavenumbers $k_j = (\partial/\partial z)\psi_j$ each satisfy the 1D electromagnetic dispersion relation $\omega_j^2 = \omega_p^2/\gamma_0 + c^2 k_j^2$, where the constant $\gamma_0 \geq 1$ parametrizes a shift in the effective plasma frequency due to transverse electron quiver. For electromagnetic waves satisfying this dispersion relation, the group velocity is approximately given by $v_g(\omega) \equiv (d/dk)\omega(k) \approx c - (c/2\gamma_0)\omega_p^2/\omega^2$. This expression evaluated at the average carrier frequency $\bar{\omega}$ defines our reference group velocity $\bar{v}_g$:

$$\bar{v}_g \equiv v_g(\bar{\omega}) \approx c\left[1 - \frac{1}{2\gamma_0}\frac{\omega_p^2}{\bar{\omega}^2}\right] \approx \frac{\bar{\omega}_2 - \bar{\omega}_1}{k(\bar{\omega}_2) - k(\bar{\omega}_1)}, \tag{3}$$

which represents the characteristic velocity at which both laser envelope modulations and Langmuir phase-fronts travel. Using the assumed vector potential, the ponderomotive force is given by

$$a^2 = \frac{1}{2}\left[|a_1|^2 + |a_2|^2 + a_1^* a_2 e^{i(\psi_2-\psi_1)} + a_1 a_2^* e^{-i(\psi_2-\psi_1)}\right]. \tag{4}$$

Since the group-velocity dispersion effects remain small in the underdense regime, linear propagation into the plasma results in a beat phase given by

$$\psi_2(z,t) - \psi_1(z,t) = \Delta\psi_0 + \int_0^{t-z/\bar{v}_g} dt'[\omega_2(t') - \omega_1(t')] + O\left(\frac{1}{\gamma_0}\frac{\omega_p^3}{\bar{\omega}^3}\frac{\omega_p L}{c}\right), \tag{5}$$

where $\Delta\psi_0$ is equal to the difference of the initial laser phases. The neglected terms limit the validity of the constant group velocity approximation to interactions lengths L less than the so-called dispersion length $L_{\mathrm{disp}} \sim (\bar{\omega}^3/\omega_p^3)(c/\omega_p)$. For accelerator applications, the useful interaction length is already limited by the dephasing length L_d, beyond which accelerated electrons cannot gain energy from the electrostatic field: $L \leq L_d \sim (\bar{\omega}^2/\omega_p^2)(c/\omega_p) \ll L_{\mathrm{disp}}$, so that our constant group velocity approximation imposes no further restriction on the interaction length.

By appropriate choice of the initial phases, we may take both a_1 and a_2 to be real. Defining the co-moving normalized beat frequency $\Delta\omega(\xi) = [\omega_2(\xi) - \omega_1(\xi)]/\omega_p$, the beat phase $\psi(\xi) = \Delta\psi(0) + \int_0^\xi d\xi'\,\Delta\omega(\xi')$, the normalized beat amplitude $\epsilon = a_1 a_2$, the average normalized intensity per laser $\bar{a}^2 = \frac{1}{2}[a_1^2 + a_2^2]$, and the electron quiver factor $\gamma_0 = \sqrt{1+\bar{a}^2}$, the slow part of the ponderomotive drive may be written as a function of ξ only:

$$a^2 = a^2(\xi) \approx \bar{a}^2 + \epsilon\cos\psi(\xi).$$

Using this form for the ponderomotive drive, the equation of motion (2) may be written as an ordinary differential equation in the co-moving coordinate ξ:

$$\frac{d^2}{d\xi^2}\phi = \phi''(\xi) = \frac{1}{2}\left[\frac{1 + \bar{a}^2 + \epsilon\cos\psi(\xi)}{(1+\phi)^2} - 1\right], \tag{6}$$

with the initial conditions $\phi(0) = \phi'(0) = 0$. Equation (6) is used for all numerical simulations discussed in Secs. IV, V, and VII, and is the starting point for our analysis of autoresonance.

III. HAMILTONIAN FORMALISM

To study autoresonance, we now develop the Hamiltonian formulation of (6). Our goal is an expression in terms of canonical action-angle variables, for which the phase-locking phenomenon is most readily analyzed. First, note that the dynamical equation for the electrostatic potential (6) can be derived from the Hamiltonian

$$\mathcal{H}(\phi,p;\xi) = \frac{1}{2}p^2 + \frac{1}{2}\left[\frac{1}{1+\phi} + \phi - 1\right] + \frac{\bar{a}^2 + \epsilon\cos\psi(\xi)}{2(1+\phi)} \equiv \mathcal{H}_0(\phi,p) + \frac{\bar{a}^2 + \epsilon\cos\psi(\xi)}{2(1+\phi)}, \tag{7}$$

with the scalar potential ϕ regarded as the generalized coordinate, $p \equiv \phi' \equiv (d/d\xi)\phi = \beta_p E_z/E_0$ regarded as the canonical momentum conjugate to ϕ, and ξ taken as the time-like evolution variable. In this way, the plasma-wave dynamics are seen to be analogous to those of a one-dimensional forced nonlinear oscillator. The component $\mathcal{H}_0$ of (7) represents the Hamiltonian of the free oscillator, involving one term $\mathcal{T}(p) = \frac{1}{2}p^2$ analogous to the kinetic energy of the oscillator (which is proportional to the electrostatic energy density of the plasma wave), and another term corresponding to an anharmonic effective potential $\mathcal{V}(\phi) = \frac{1}{2}[1/(1+\phi) + \phi - 1]$. The remaining driving term $\mathcal{H}(\phi,p;\xi) - \mathcal{H}_0(\phi,p)$ corresponds to the time-dependent forcing of the oscillator.

In the absence of forcing (i.e., $\epsilon = \bar{a}^2 = 0$), the dynamics governed by $\mathcal{H}_0(\phi,p) = \mathcal{T}(p) + \mathcal{V}(\phi)$ are conservative, so the oscillator energy, i.e., the value H of the Hamiltonian $\mathcal{H}_0$

along any particular unperturbed orbit, remains constant. In the physically allowed region $\phi > -1$, the effective potential $\mathcal{V}(\phi)$ is non-negative and possesses a single minimum $\mathcal{V}(0)=0$, while $\mathcal{V}(\phi)\to\infty$ as $\phi\to -1^+$ or $\phi\to\infty$. So for any value of energy $H\geqslant 0$, there exists a phase space trajectory $[\phi(\xi;H),p(\xi;H)]$ which is a closed periodic orbit.

Making a canonical transformation to the action-angle variables of the free oscillator, $\phi=\phi(\mathcal{I},\theta)$, $p=p(\mathcal{I},\theta)$, we can express (7) as

$$\mathcal{H}(\mathcal{I},\theta;\xi) = \mathcal{H}_0(\mathcal{I}) + \frac{\bar{a}^2+\epsilon\cos\psi(\xi)}{2[1+\phi(\mathcal{I},\theta)]}, \tag{8}$$

where the action $\mathcal{I}$ is defined in terms the area in phase space contained within the unperturbed orbit $[\phi(\xi;H),\phi'(\xi;H)]$ of energy H:

$$\mathcal{I} \equiv \frac{1}{2\pi}\oint p\,d\phi = \frac{1}{\pi}\int_{\phi_-}^{\phi_+}\phi'\,d\phi. \tag{9}$$

Here, ϕ_+ and ϕ_- are the upper and lower turning points of the orbit, respectively, given by $\phi_\pm = H\pm\sqrt{H^2+2H}$, and we have used symmetry to reduce the integration path in (9) to the segment where $p\geqslant 0$. By making the change of variables $\phi=\phi_+-(\phi_+-\phi_-)\sin^2(u)$, the action (9) can be calculated using a standard integral table:[30]

$$\mathcal{I} = \frac{2(\phi_+-\phi_-)^2}{\pi\sqrt{1+\phi_+}}\int_0^{\pi/2} du\frac{\sin^2(u)\cos^2(u)}{\sqrt{1-\frac{\phi_+-\phi_-}{1+\phi_+}\sin^2(u)}}$$
$$= \frac{4}{3\pi}\left[1+H-\sqrt{H^2+2H}\right]^{1/2} \times\left\{\frac{(1+H)E(\kappa)}{1+H-\sqrt{H^2+2H}} - K(\kappa)\right\}. \tag{10}$$

Here, $K(\kappa)$ and $E(\kappa)$ are complete elliptic integrals of the first and second kind, respectively, whose modulus satisfies $\kappa^2=[2(1+H)\sqrt{H^2+2H}-2H(2+H)]$. At this point, one could in principle use (10) to find $\mathcal{H}_0(\mathcal{I})$, but fortunately, such a cumbersome inversion will not be necessary. The normalized (i.e., dimensionless) nonlinear frequency $\Omega(H)$ of the unforced oscillator is given by

$$\Omega(H) = \left(\frac{\partial\mathcal{I}}{\partial H}\right)^{-1} = \frac{\pi}{2}\frac{[1+H-\sqrt{H^2+2H}]^{1/2}}{E(\kappa)}. \tag{11}$$

To put (7) in the desired form (8), the remaining ingredient needed is the canonical transformation $\phi=\phi(\mathcal{I},\theta)$. An explicit formulation of this will also not be needed, and we may proceed by formally assuming that we have made this substitution. Then, $\phi=\phi(\mathcal{I},\theta)$ is a periodic function of θ, and we can expand the driving term appearing in (8) in a Fourier series as

$$\frac{\bar{a}^2+\epsilon\cos\psi(\xi)}{2[1+\phi(\mathcal{I},\theta)]} = [\bar{a}^2+\epsilon\cos\psi(\xi)]\sum_{n=-\infty}^{\infty} b_n(\mathcal{I})e^{in\theta}. \tag{12}$$

Because (12) is a real-valued function, the Fourier coefficients must satisfy $b_n=b^*_{-n}$, and are defined by

$$b_n(\mathcal{I}) = \frac{1}{2\pi}\int_0^{2\pi} d\theta\frac{e^{-in\theta}}{2[1+\phi(\mathcal{I},\theta)]}. \tag{13}$$

We put (13) into a form more amenable to calculation by changing variables using $\theta=\Omega(H)\xi$, and integrating over one period $0\leqslant\xi\leqslant\Xi\equiv 2\pi/\Omega$ of the co-moving coordinate. Furthermore, if we choose the origin of the orbit associated with the energy H, such that $\phi(\xi=0;H)=\phi_+$, the potential $\phi(\xi;H)$, and hence $[1+\phi(\xi;H)]^{-1}$, are symmetric about the point $\xi=\Xi/2$. Since the imaginary parts of (13) are obtained by integrating over the antisymmetric functions $\sin(n\Omega\xi)$, the b_n values are purely real and are given by

$$b_{\pm n}(H) = b_{\pm n}(H)^* = \frac{1}{\Xi(H)}\int_0^{\Xi(H)} d\xi\frac{\cos[n\Omega(H)\xi]}{2[1+\phi(\xi;H)]}.$$

Up to this point, no approximations have been made in the canonical transformations to the action-angle variables of the unforced oscillator. Now, we make the single resonance approximation[31] (SRA) to (8), by assuming that the rapidly oscillating terms of the Hamiltonian average to zero and contribute negligibly to the dynamics. Anticipating the developments of Sec. IV, we realize that under certain frequency-locking conditions derived there, autoresonant excitation occurs, wherein the plasma wave amplitude, or equivalently, the free-oscillator energy $H(\xi)=\mathcal{T}(\phi'(\xi))+\mathcal{V}(\phi(\xi))$, grows secularly such that the dynamical frequency $\Omega(\xi)$ of the forced oscillator approximately matches that of the unforced oscillator at that same amplitude, $\Omega(\xi)\approx\Omega(H(\xi))$. Simultaneously, this instantaneous oscillator frequency follows that of the driving beat frequency of the wave, $\Omega(\xi)\approx\Delta\omega(\xi)$. Under these assumptions, we can consistently neglect all terms in the sum (12) except the constant term or those terms with frequency dependence $\sim\pm[\Omega(\xi)-\Delta\omega(\xi)]$. The averaged Hamiltonian then becomes

$$\mathcal{H}(\mathcal{I},\theta;\xi) = \mathcal{H}_0(\mathcal{I}) + \epsilon b_1(\mathcal{I})\cos[\theta-\psi(\xi)] + \bar{a}^2 b_0(\mathcal{I}).$$

We now make an explicitly ξ-dependent canonical transformation to the rotating action-angle variables $(\hat{\mathcal{I}},\Psi)$. Using the mixed-variable generating function $F_2(\hat{\mathcal{I}},\theta;\xi)=[\theta-\psi(\xi)]\hat{\mathcal{I}}$, our old and new coordinates are related by $\Psi=\partial F_2/\partial\hat{\mathcal{I}}=\theta-\psi(\xi)$ and $\mathcal{I}=\partial F_2/\partial\theta=\hat{\mathcal{I}}$. Dropping the caret from the new action, the Hamiltonian in the rotating frame is

$$\mathcal{K}(\mathcal{I},\Psi;\xi) = \mathcal{H}_0(\mathcal{I}) - \Delta\omega(\xi)\mathcal{I} + \epsilon b_1(\mathcal{I})\cos\Psi + \bar{a}^2 b_0(\mathcal{I}).$$

The resulting SRA canonical equations of motion are

$$\frac{d}{d\xi}\Psi = \Omega(\mathcal{I}) - \Delta\omega(\xi) + \epsilon\frac{\partial b_1}{\partial\mathcal{I}}\cos\Psi + \bar{a}^2\frac{\partial b_0}{\partial\mathcal{I}}, \tag{14a}$$

$$\frac{d}{d\xi}\mathcal{I} = \epsilon b_1(\mathcal{I})\sin\Psi, \tag{14b}$$

for which we next determine the required conditions for phase-locking.

IV. AUTORESONANT RESPONSE

The essential ingredients for autoresonance are: a nonlinear, oscillatory degree of freedom (in our case, the plasma wave) evolving, in the absence of any forcing, within an integrable region of phase space; a continuous functional relationship between the nonlinear frequency and energy of the oscillation possessing a well-defined linear limit; an applied oscillatory driving force (in our case, the modulated ponderomotive envelope of the lasers) which can be considered perturbative, so that the notion ofthe nonlinear frequency of the unforced oscillator remains meaningful; and initial conditions and forcing profile consistent with adiabatic passage through resonance (APTR)—namely, an initially unexcited system (quiescent plasma), and an initial drive frequency appropriately far from the linear resonance, with subsequent time dependence that is sufficiently slowly varying but otherwise arbitrary.

The key consequence of autoresonant beat-wave generation is the robust entrainment between the three relevant frequencies: the beat frequency $\Delta\omega(\xi)$ of the driving lasers, the instantaneous frequency $\Omega(\xi)$ of the driven plasma wave, and the nonlinear frequency $\Omega(H)$ of the unforced plasma wave. Assuming this phase-locking is achieved, amplitude control of the plasma wave can be simply understood via (11): because the frequency of the freely evolving nonlinear plasma wave is a function of the energy, phase-locking of the driven wave to the envelope such that $\Delta\omega(\xi)\approx\Omega(\xi)\approx\Omega(H)$ implies that changing the drive frequency will correspondingly change the oscillator energy. In our case, (11) indicates that $\Omega(H)$ is a decreasing function of H, so that in order to increase the plasma wave amplitude, one must decrease the beat frequency as a function of ξ.

While we have indicated how autoresonance can lead to large plasma waves, we have not yet shown under what conditions such phase-locking occurs. To address this question, we first consider the linear and weakly nonlinear response, valid for moderate Langmuir amplitudes. Next, we consider the fully nonlinear case, for which we derive adiabaticity requirements for autoresonance.

A. Small-amplitude response and phase-locking

When the drive is first applied with its frequency above the linear resonance, the plasma wave amplitude [and, hence, H and $\mathcal{I}(H)$] are small and we can linearize Eqs. (14a) and (14b). In this limit, the oscillator is harmonic, with $\Omega(H)=1$, $\phi(\xi)=\sqrt{2H}\cos(\xi)$, and $H=\mathcal{I}$, so that $b_0=-\frac{1}{2}H$, $b_1=\sqrt{2H}/4$, and Eqs. (14) become

$$\frac{d}{d\xi}\Psi = 1-\frac{1}{2}\bar{a}^2-\Delta\omega(\xi)+\frac{\epsilon}{4\sqrt{2}}\frac{1}{\sqrt{\mathcal{I}}}\cos\Psi, \tag{15a}$$

$$\frac{d}{d\xi}\mathcal{I} = \frac{\epsilon}{2\sqrt{2}}\sqrt{\mathcal{I}}\sin\Psi. \tag{15b}$$

Note that the $(1-\frac{1}{2}\bar{a}^2)$ contribution to $(d/d\xi)\Psi$ corresponds, in normalized units, to the leading-order expansion of the effective plasma frequency in the electromagnetic dispersion relation

$$\omega_{p_{\text{eff}}}\equiv\omega_p/\gamma_0=\omega_p/\sqrt{1+\bar{a}^2}\approx\omega_p\left(1-\frac{1}{2}\bar{a}^2+\cdots\right),$$

which is shifted from the bare value ω_p due to the transverse quiver motion of the electrons in the applied laser fields. Physically, this implies that one must ensure that the drive frequency begins sufficiently far above, and then is slowly swept past, the effective frequency $\omega_{p_{\text{eff}}}$, rather than the bare frequency ω_p. One may wonder why only the leading-order correction appears here, while we never explicitly invoked any small-a^2 approximation. This is because when making the SRA, we ignored terms of the form $\bar{a}^2e^{in\theta}$ for $|n|\geqslant 1$, while such terms can appreciable effect the dynamics for large intensity $\bar{a}^2$ despite being off-resonance.

For the driven plasma wave, we have $\Delta\omega(\xi)\sim\Omega(\xi)\sim 1$, while we seek solutions for which $|\Delta\omega(\xi)-\Omega(\xi)|\ll 1$ as a result of special initial and forcing conditions: an initially unperturbed plasma, $\phi(\xi=0)=\phi'(\xi=0)=0$; an initial tuning of the beat frequency above resonance, i.e., $\Delta\omega(\xi=0)>\omega_{p_{\text{eff}}}$, and subsequently a slow downward frequency chirp through resonance, where the chirp rate is be characterized by a parameter $\alpha\equiv\alpha(\xi)\equiv-(d/d\xi)\Delta\omega(\xi)$, with $0\leqslant\alpha\ll 1$.

For a linear frequency chirp around the effective plasma frequency,

$$\Delta\omega(\xi)=1-\tfrac{1}{2}\bar{a}^2-\alpha\xi, \tag{16}$$

the simple harmonic oscillator equations (15) have analytic solutions in terms of the Fresnel sine and cosine integrals.[32] We briefly summarize the extensive characterization of these solutions found in Ref. 24. When the drive is first applied far from resonance, the oscillator response can be divided into two components: one ringing component precisely at $\omega_{p_{\text{eff}}}$, and the other at the driving frequency $\Delta\omega(0)$, both of small amplitude. The singular term $\sim\mathcal{I}^{-1/2}$ in (15a) allows for a large change in phase at small amplitude without violating the requirement that $\phi(\xi)$ remain smooth, so that the response at the driven frequency can adjust itself to the drive, and phase-locking can occur. As the frequency is swept toward the resonance, these driven, phase-locked oscillations grow. Meanwhile, the response at the resonant frequency has no such phase relation with the drive, and remains small. In this way, we essentially have one growing, phase-locked plasma wave when the drive frequency reaches the resonant frequency.

As the resonance is approached, the amplitude of the plasma wave begins to become large and one must account for the growing nonlinearities. We therefore expand the expression for the free nonlinear frequency (11) to first order: $\Omega(H)=1-\frac{3}{8}H=1-\frac{3}{8}\mathcal{I}$, and continue to use the linearized frequency chirp (16). Making the change of variable $\mathcal{A}\equiv 4\sqrt{2\mathcal{I}}$, we have

$$\frac{d}{d\xi}\Psi = \alpha\xi - \frac{3}{256}\mathcal{A}^2 + \frac{\epsilon}{\mathcal{A}}\cos\Psi,$$
$$\frac{d}{d\xi}\mathcal{A} = \epsilon \sin\Psi. \tag{17}$$

This set of equations can be reduced to a single first-order ordinary differential equation by defining the complex dynamical variable $Z \equiv -\sqrt{256/3\alpha}\mathcal{A}e^{i\Psi}$, a re-scaled independent variable $\zeta \equiv \sqrt{\alpha}\xi$, and the dimensionless parameter $\mu \equiv \epsilon\sqrt{3/(256\alpha^{3/2})}$, to obtain

$$i\frac{d}{d\zeta}Z + (\zeta - |Z|^2)Z = \mu. \tag{18}$$

Thus, the weakly nonlinear problem is now described by a dynamical equation with a single parameter μ that combines the drive strength ϵ and the chirp rate α. It has been found numerically[33] that the solution to (18) has a bifurcation at the critical value $\mu = \mu_c \approx 0.411$. For $\mu < \mu_c$, the plasma wave response quickly dephases from the drive, resulting in only small excitations. In contrast, for $\mu > \mu_c$, phase-locking occurs and the plasma wave can grow to large amplitude. This critical behavior with respect to μ translates into a critical drive strength ϵ and chirp rate α for the nonlinear oscillator to be autoresonantly excited. The condition is

$$\alpha \leq \left(\frac{3\epsilon^2}{256\mu_c^2}\right)^{2/3} \approx 0.169\epsilon^{4/3}. \tag{19}$$

Thus, for a given laser intensity, one can readily find the maximum chirp rate that can be tolerated and still obtain high-amplitude plasma waves. We demonstrate the sensitivity of this critical behavior for three drive strengths in Fig. 1, which plots numerical results from the full quasi-static equation of motion (6). Plot (a) shows the dependence of the chirp rate of the maximum amplitude about the critical chirp rate α_c. Plot (b) demonstrates the dynamic frequency-locking that occurs in autoresonance for $\epsilon = 0.005$, and compares this to the case in which autoresonance fails to occur.

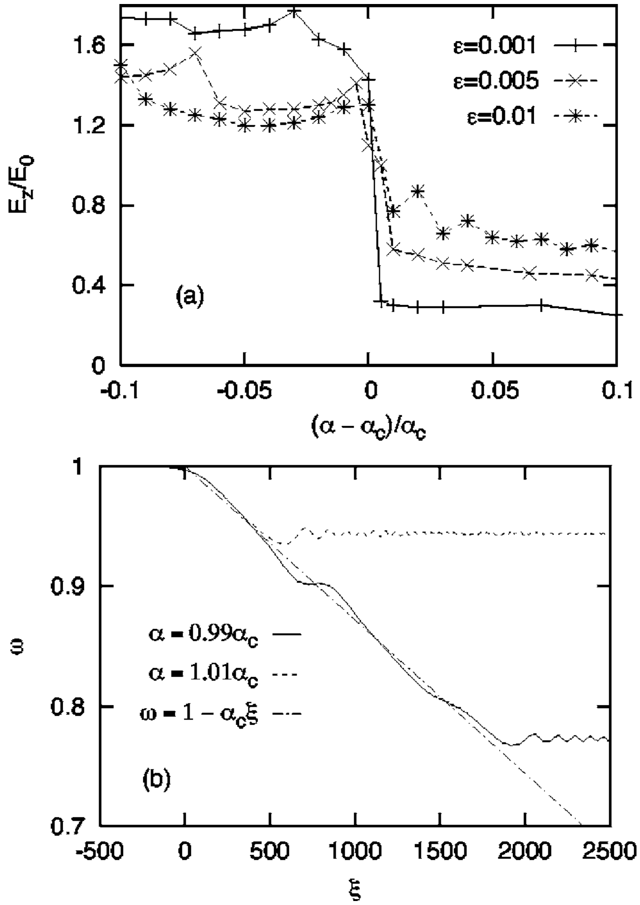

FIG. 1. Demonstration of the critical autoresonant behavior. In (a), we see that chirp rates slightly below α_c grow above linear wave-breaking, while chirps a tiny fraction too large saturate below E_0. (b) compares the phase locking in autoresonance (solid line) to that of nonautoresonant behavior (dashed line) for $\epsilon = 0.005$. The critical drive (mixed line) is included for reference.

B. Fully nonlinear autoresonant response

If phase-locking is maintained through the weakly nonlinear regime, the amplitude continues to grow and one must consider further nonlinearities beyond those included in (18). In this case, there arises more stringent restrictions on the chirp rate for adiabatic phase-locking to persist. We calculate this condition by first finding a second-order equation for the phase Ψ. Taking the time derivative of (14a), the phase Ψ is seen to obey the following second-order equation:

$$0 = \frac{d^2}{d\xi^2}\Psi + \epsilon\frac{\partial b_1}{\partial \mathcal{I}}\sin\Psi\frac{d}{d\xi}\Psi + \frac{d}{d\xi}\Delta\omega$$
$$- \epsilon b_1(\mathcal{I})\sin\Psi\left[\frac{\partial\Omega}{\partial\mathcal{I}} + \bar{a}^2\frac{\partial^2 b_0}{\partial\mathcal{I}^2} + \epsilon\frac{\partial^2 b_1}{\partial\mathcal{I}^2}\cos\Psi\right]. \tag{20}$$

Now, we assume (see, e.g., Ref. 34) that the free action can be written as

$$\mathcal{I} = \mathcal{I}_0 + \Delta\mathcal{I}, \tag{21}$$

where $\mathcal{I}_0 = \mathcal{I}_0(\xi)$ is the slowly varying, secularly evolving action about which there are small oscillations given by $\Delta\mathcal{I} = \Delta\mathcal{I}(\xi)$. These oscillations correspond to fluctuations in Ψ about its (slowly varying) phase-locked value $\bar{\Psi} = \bar{\Psi}(\xi)$, an example of which can be seen in Fig. 1(b). In the autoresonant case (solid line), we see that as the plasma wave is excited, its frequency does indeed make small oscillations about the drive frequency.

Using the form (21) for the action, the lowest-order equation for the phase is identical to (20), with $\mathcal{I}$ being replaced everywhere by $\mathcal{I}_0$. In this way, the phase itself is seen to obey a nonlinear oscillator equation, with an effective nonlinear damping term, and a conservative "forcing," described by the terms on the second line, which is derivable from an effective "potential" whose shape is dictated by the slowly evolving action $\mathcal{I}_0$ and the drive parameters ϵ and α. Phase-locking then corresponds to trapping of Ψ in a basin of this effective potential about $\bar{\Psi}$, such that the nonconservative term on the first line must either provide damping or remain small if excitatory. Typically, the ratio of this nonconservative term to the second term in the conservative force is given by

$$\left(\frac{1}{b_1}\frac{\partial b_1}{\partial \mathcal{I}_0}\frac{\partial \Omega}{\partial \mathcal{I}_0}\right)\left(\frac{d\Psi}{d\xi}\right) \sim \left(\frac{1}{b_1}\frac{\partial b_1}{\partial \Omega}\right)\left(\frac{d\Psi}{d\xi}\right) \sim \frac{d\Psi}{d\xi} \ll 1$$

because the nonlinear phase oscillations are slow compared to ω_p.

Actually, over most of the typical range of parameter values, the last two terms in the conservative forcing are small compared to the first two terms, and one can understand the dynamics of the phase oscillations using the "biased" pendulum equation $(d^2/d\xi^2)\Psi \approx \alpha + [\epsilon b_1(\mathcal{I}_0)\partial\Omega/\partial\mathcal{I}_0]\sin\Psi$, although we will continue to work with the full equation (20). Clearly, for a given $\mathcal{I}_0$, if the normalized chirp rate α remains sufficiently small compared to the normalized drive strength ϵ, then the effective potential will be of the tilted-washboard variety, with a series of periodically spaced local minima in Ψ at intervals of 2π. As α increases, the depth of these wells decreases, until they finally disappear, as does any opportunity for phase-locking.

Thus, a necessary condition for trapping is that the effective force can actually vanish at some fixed point $\bar{\Psi}$:

$$\alpha(\xi) + \epsilon b_1(\mathcal{I}_0)\sin\bar{\Psi}\left[\frac{\partial\Omega}{\partial\mathcal{I}_0} + \bar{a}^2\frac{\partial^2 b_0}{\partial\mathcal{I}_0^2} + \epsilon\frac{\partial^2 b_1}{\partial\mathcal{I}_0^2}\cos\bar{\Psi}\right] = 0. \quad (22)$$

For given $\mathcal{I}_0$, this determines the average, slowly varying phase $\bar{\Psi}$ about which trapping occurs. In the linear ($\mathcal{I}_0 \to 0$), weakly forced ($0 \leq \epsilon \lll 1$) or weakly chirped ($\alpha \to 0^+$) regimes, this phase value is known[24] to be $\bar{\Psi} \approx \pi$, but for nonlinear plasma waves, stronger forcing, or faster chirping, this phase can shift appreciably. Since $|\sin\bar{\Psi}|$, $|\cos\bar{\Psi}| \leq 1$, Eq. (22) also imposes an upper bound on the frequency chirp $\alpha(\xi)$ for which the phase can remain trapped in autoresonance, regardless of the actual value of the phase at which locking occurs. Setting $|\sin\bar{\Psi}| = |\cos\bar{\Psi}| = 1$ above, we obtain an upper bound on α beyond which any phase-locking is impossible:

$$\alpha(\xi) \leq \epsilon|b_1(\mathcal{I}_0)|\left[\left|\frac{\partial\Omega}{\partial\mathcal{I}_0}\right| + \bar{a}^2\left|\frac{\partial^2 b_0}{\partial\mathcal{I}_0^2}\right| + \epsilon\left|\frac{\partial^2 b_1}{\partial\mathcal{I}_0^2}\right|\right]. \quad (23)$$

Again, for realistic parameters, the force balance typically resides predominately between the first two terms in (22), and hence this upper bound, although approximate, is expected to provide a reasonably tight cutoff for autoresonant phase-locking, which has been confirmed by numerical simulation. This inequality can also be thought of as giving the maximum achievable plasma wave amplitude (implicitly as a function of $\mathcal{I}_0$) for a given chirp rate and laser power. We show the dependence of the saturated longitudinal field on the chirp rate as a solid line in Fig. 2(a) for a number of different drive strengths. For a fixed drive strength ϵ, the maximum attainable electric field jumps discontinuously at the critical chirp rate α_c given by (19). The dotted lines correspond to solutions of (23) that cannot be accessed when

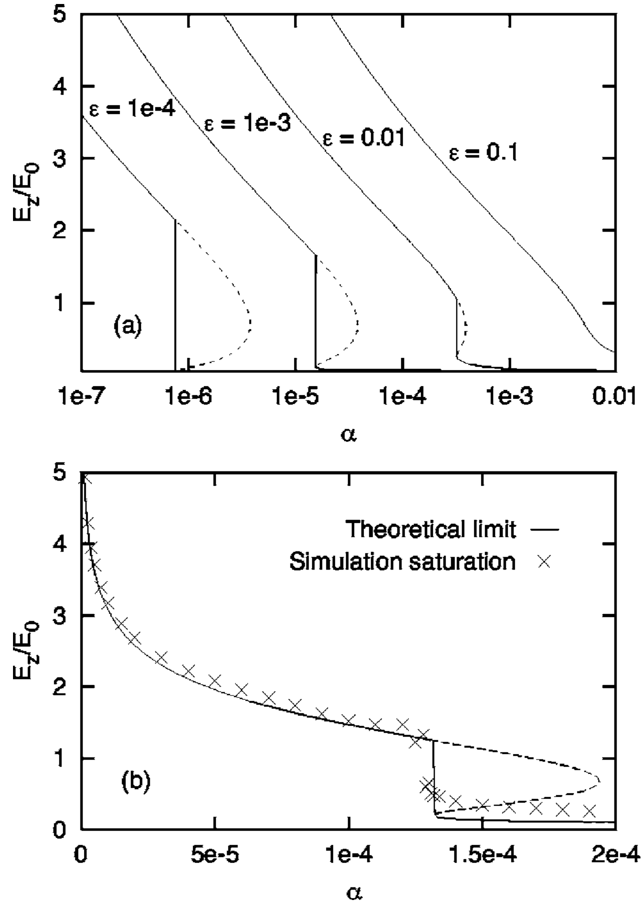

FIG. 2. Shows the maximum plasma wave amplitude obtainable before the "slowness" condition (23) is violated. In (a), we plot the maximum longitudinal field as a function of the chirp rate for four different driving strengths. Dotted lines indicate hysteresis at α_c given by (19). Panel (b) compares the theory (line) with numerically determined saturation for ϵ=0.005.

starting from vanishing initial longitudinal field, and as such constitutes a form of hysteresis in the excitation; the solid lines show the stable branches for the case of interest. Figure 2(b) shows a comparison of the theoretical maximum amplitude and that found by numerically integrating the quasistatic equation of motion (6) for ϵ=0.005.

Asymptotic expansions and numerical plots for $\Omega(\mathcal{I})$ and $b_n(\mathcal{I})$ reveal that the right-hand-side of (23) decreases with increasing $\mathcal{I}_0$ beyond moderate values of $\mathcal{I}_0$. Thus, the adiabatic nonlinear phase-locking condition (23) become increasingly stringent, and the growing plasma wave eventually falls out of frequency-locking. Mathematically, this saturation can be traced to the nonlinear nature of the forcing in (6), where the effective strength depends both on the external drive intensity and the plasma wave amplitude; physically, to the fact that as the plasma wave grows, the electrons become increasingly relativistic and therefore less susceptible to displacement via the ponderomotive forcing.

As a result of relativistic detuning, recall that in the original RL/TD scheme, the plasma wave amplitude exhibits slow (compared to ω_p^{-1}) nonlinear modulations that appear as beating; i.e., periodic amplitude oscillations up to the RL limit and back to a nearly unexcited state. As the wave is driven to a high amplitude, its phase slowly slips until it is more than $\sim\pi/2$ out of phase with respect to the laser beat and then gives its energy back to the lasers, then continues to shift further out of phase, only to be re-excited when its amplitude approaches zero and it can re-establish phase matching with the drive.

In the DMG scheme, the plasma wave amplitude not only can peak at a higher maximum than in the original scheme, but typically will sustain a higher average value at long times, exhibiting a nonlinear ringing about some non-zero saturated value. In this case, when the frequency locking fails the wave phase is closer to its neutral value with respect to energy exchange with the drive, and the frequency difference and phase lag then grow secularly in time. Depending on initial parameters, the growth to the absolute maximum can either be essentially monotonic, or exhibit intermittent plateaus or dips between periods of resumed growth, before finally leveling off.

In our autoresonant scheme based on APTR, the behavior more closely resembles that in DMG scheme, but exhibits more nearly monotonic growth, higher peak fields, and less ringing after saturation. The extent of the amplitude and phase excursions is determined by how deeply the phase is trapped in its effective potential well. This in turn depends both on how steep and how deep is the available well (determined by the Langmuir amplitude and drive lasers parameters), and to what extent the phase can be nudged near the bottom of the well and kept there (determined by the initial conditions and the adiabaticity of the chirped forcing). Numerical simulations suggest that the depth of this trapping is improved by using a stronger drive, starting the drive frequency further above resonance, and chirping more slowly. In practice, of course, each of these strategies involves trade-offs. Increasing the drive strength increases the growth rates for laser-plasma instabilities that might disrupt the forcing. Either increasing the initial frequency up-shift or decreasing the chirp rate decreases the final amplitude that can be reached during a fixed interaction time.

V. EXPERIMENTAL CONSIDERATIONS

Unfortunately, as has been alluded to previously, the PBWA does not have unlimited time to be excited, as deleterious instabilities will eventually destroy wave coherence. For the parameters of interest, the oscillating two-stream (also referred to as modulational) instability limits the lifetime of coherent Langmuir waves to the ion time scale, i.e., for times of the order of a few $1/\omega_i$. Although it is possible that the growth of this instability may be mitigated somewhat by the use of a chirped laser, in this paper, we will use as a conservative figure the results of Mora *et al.*[11] to set the time limit during which we can excite a coherent plasma wave suitable for accelerator applications.

For the relatively cold plasmas and moderately intense lasers we consider, it is shown in Ref. 11 that the growth rate of the oscillating two-stream instability is approximately equal to ω_i, and that this instability impedes plasma wave excitation and destroys coherence after about five e-foldings. Thus, we see that the drive lasers should have time duration $T\lesssim 5/\omega_i$. If one chirps the drive frequency leading to a total shift $\delta\omega$ during the autoresonant excitation, then the normalized chirp rate is limited to

$$\alpha \gtrsim 0.2\frac{\omega_p}{\omega_i}\frac{\delta\omega}{\omega_p}, \tag{24}$$

or approximately $\alpha\gtrsim 2.3\times10^{-3}\delta\omega/\omega_p$ for singly ionized helium. Below, we choose two experimentally relevant parameter sets, one corresponding to a 10 μm CO_2 laser; the other, to a 800 nm chirped pulse amplification[35] (CPA) Ti:sapphire laser system. We demonstrate how, beginning with the laser frequency above the linear resonance and then slowly decreasing it, one can robustly excite plasma waves to amplitudes larger than the cold, linear wave-breaking limit in times commensurate with onset of the oscillating two-stream instability.

A. CO_2 Laser at 10 μm

We first consider parameters roughly corresponding to the most recently published UCLA upgrade.[14] We assume two pulses of duration $T=100$ ps that enter the plasma at $t=0$, whose central wavelengths of 10.27 and 10.59 μm imply a resonant plasma density $n_0\approx 1\times10^{16}$ cm^3. The lasers have normalized intensities $a_1=a_2=0.14$, corresponding to a normalized drive strength $\epsilon=0.02$, so the threshold condition (19) implies that the normalized chirp rate should satisfy $\alpha(t)=-(d/dt)\Delta\omega(t)/\omega_p<0.0009$. We choose a linear chirp, so that in physical units the beat frequency is given by $\Delta\omega(t)=(\mu_0+\alpha\omega_p t)$, where $\mu_0=1.15$ and $\alpha=0.000\,65$, with a total frequency sweep from $\Delta\omega(t=0)=1.15$ to $\Delta\omega(t=T)=0.74$. For these parameters, we collect the results from simulations integratingthe quasi-static equation of motion (6) in Fig. 3. Figure 3(a) demonstrates the excitation of a uniform accelerating field E_z of 10 GV/m, which is above the linear, cold, wave-breaking limit of $E_0\approx 8.8$ GV/m, but below the cold relativistic limit $E_{\rm WB}\approx 61$ GV/m. The total chirp is modest, only about 1.5% of the laser carrier frequency $2\pi c/\lambda$.

For comparison, we also plot the simulated envelopes of the longitudinal field for the resonant RL/TD case $\Delta\omega(t)=\Delta\omega(0)=1$, and for the chirped DMG scheme starting on linear resonance, $\Delta\omega(t)=(1-\alpha\omega_p t)$, but using the same chirp rate as above. The resonant case demonstrates the characteristic RL limit of $E_z\leqslant E_{\rm RL}=(16\epsilon/3)^{1/3}E_0\approx 4.2$ GV/m, whereas the DMG scheme fails to achieve appreciable dynamic phase-locking, and the final plasma wave amplitude is about the same as in the resonant (unchirped) case. Using approximately these parameters, UCLA experiments have inferred accelerating amplitudes up to 2.8 GV/m[13] over short regions of plasma. More recently, plasma density variations corresponding to $E_z\approx 0.2-0.4$ GV/m have been directly measured with Thomson scattering.[36]

Perhaps more important than the higher-amplitude field in the autoresonant APTR case, is the fact that excitation is very robust with respect to mismatches between the beat frequency and the plasma frequency. In practice, these mismatches inevitably result from limited diagnostic accuracy or shot-to-shot jitter in the plasma or laser parameters. Because one sweeps over a reasonably broad frequency range and one

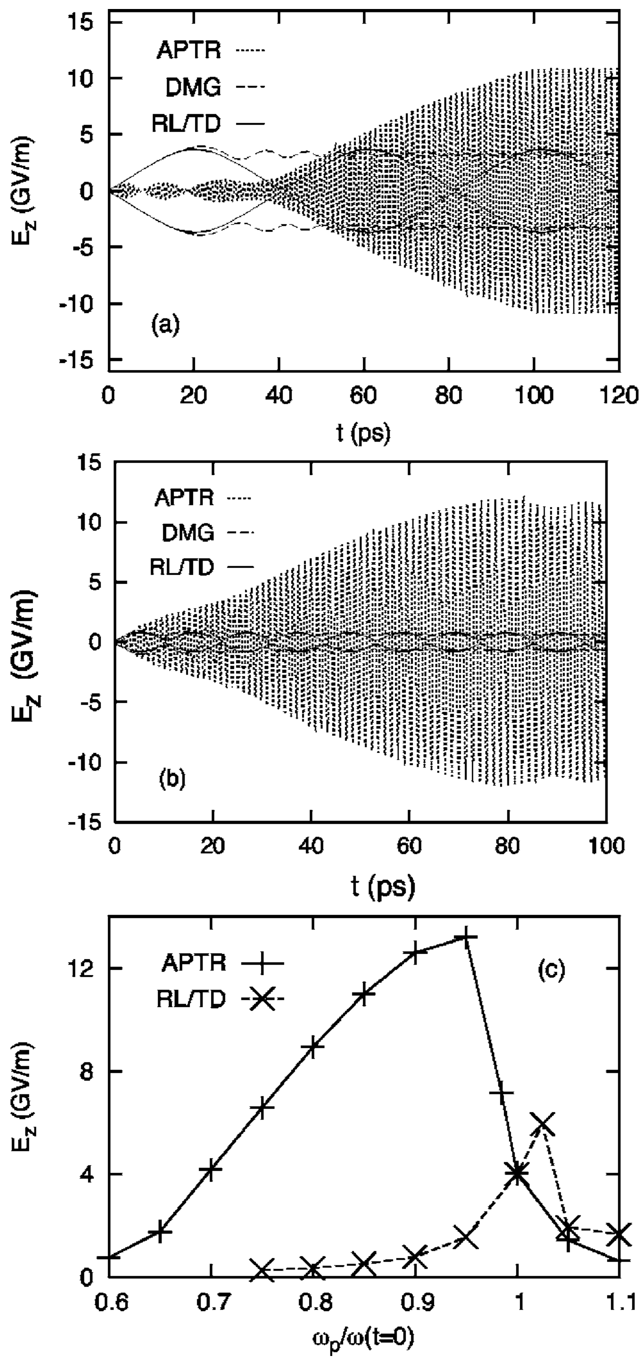

FIG. 3. Plasma wave excitation for a 10 μm CO_2 laser with intensity 2.7 $\times 10^{14}$ W/cm^2 (ϵ=0.02). In (a), the APTR case has $\omega(0)=1.15\omega_p$, and $\omega=\omega_p$ at $t\approx 40$ ps (α=0.000 65). Total chirp is 1.5% of laser frequency. For comparison, we include the envelopes with no chirp, and DMG chirp starting on resonance. Panel (b) is the same as (a), with ω_p changed by 10%. Panel (c) demonstrates robust field excitations of 5–10 GV/m for density errors of order ±20% for APTR, while the traditional PBWA only effectively excites E_z near resonance.

only needs to pass through the resonance at some indeterminate point during the chirp history, no precise matching is required, and the exact value of the plasma density need not be accurately known. This robustness is demonstrated in Figs. 3(b) and 3(c). Plot (b) shows the longitudinal field profile attained when there is a 10% variation in the density, demonstrating that APTR yields uniform, large-amplitude fields, while forcing the plasma wave off-resonance yields small accelerating gradients. In Fig. 3(c), we plot the final accelerating gradient achieved via APTR when we vary the value of ω_p over a range of ±10%, from its "design" value, while keeping the laser parameters fixed. We see large levels of excitation for a wide range in plasma variation, corresponding roughly to density mismatch/errors up to 20%. On the other hand, the traditional PBWA scheme only significantly excites the Langmuir waves for plasma densities such that the resonance condition is nearly met. Thus, not only is autoresonant plasma wave excitation effective in avoiding saturation from detuning, it also mitigates experimental uncertainties in or shot-to-shot variations of plasma density.

B. Ti:sapphire laser at 800 nm

In this section, we analyze a representative case for a Ti:sapphire CPA laser in a singly ionized He plasma, with $n_0=1.4\times 10^{18}$ cm^{-3}, so that $\omega_p/\bar{\omega}=1/25$, and a laser duration $T=3.2$ ps, chosen to correspond to the modulational instability limit. If we consider two 2-J pulses compressed to this time duration and focused to a waist of $w_0\approx 30$ μm, this implies intensities of $I_0=2.0\times 10^{17}$ W/cm^2, so that with the laser wavelength $\lambda\approx 800$ nm, we have $a_1=a_2=0.3$, and $\epsilon=0.09$. We choose $\Delta\omega(t=0)=1.2$, $\Delta\omega(t=T)=0.5$, for a normalized chirp $\alpha=0.0025$. The resulting plasma wave excitation is shown in Fig. 4(a). Here, we see maximum longitudinal electric fields $E_z\approx 260$ GV/m, corresponding to $\sim 1.6E_0\approx 0.25E_{\mathrm{WB}}$. For comparison, we also plot the resonant case, for which detuning results in maximum fields corresponding to the familiar RL limit $(16\epsilon/3)^{1/3}E_0 \approx 125$ GV/m, and the DMG case (starting on-resonance), which yields results similar to the APTR case. The distinction between passing through resonance and starting on-resonance can be seen, however, in Fig. 4(b), for which DMG scheme starting on-resonance does not experience the fortuitous frequency-locking, as in case (a). In contrast, Fig. 4(b) shows that the uniform accelerating fields obtained via APTR are only slightly affected by the change in the resonant plasma frequency. Finally, Fig. 4(c) shows the robustness of autoresonant excitation, for which density imperfections of ±35% have little effect on the accelerating gradients achieved.

VI. FLUID SIMULATIONS

In order to apply the formalism developed for autoresonant excitation, we have made a series of simplifying assumptions to arrive at the driven, nonlinear ordinary differential equation (6). Namely, we have assumed 1D dynamics, quasi-static plasma response, and neglected laser evolution. To test the latter two assumptions and to validate some of our conclusions using a more faithful laser-plasma model, we have simulated the experimental parameters of Sec. V using a fully relativistic, Maxwell-fluid code in 1D.[37] This code solves the cold electron fluid equations coupled to Maxwell's equations in a frame moving at the speed of light c.

The accelerating electric fields obtained in the fluid simulations for the resonant RL/TD PBWA, the DMG chirp from resonance, and the APTR chirp are included in Fig. 5.

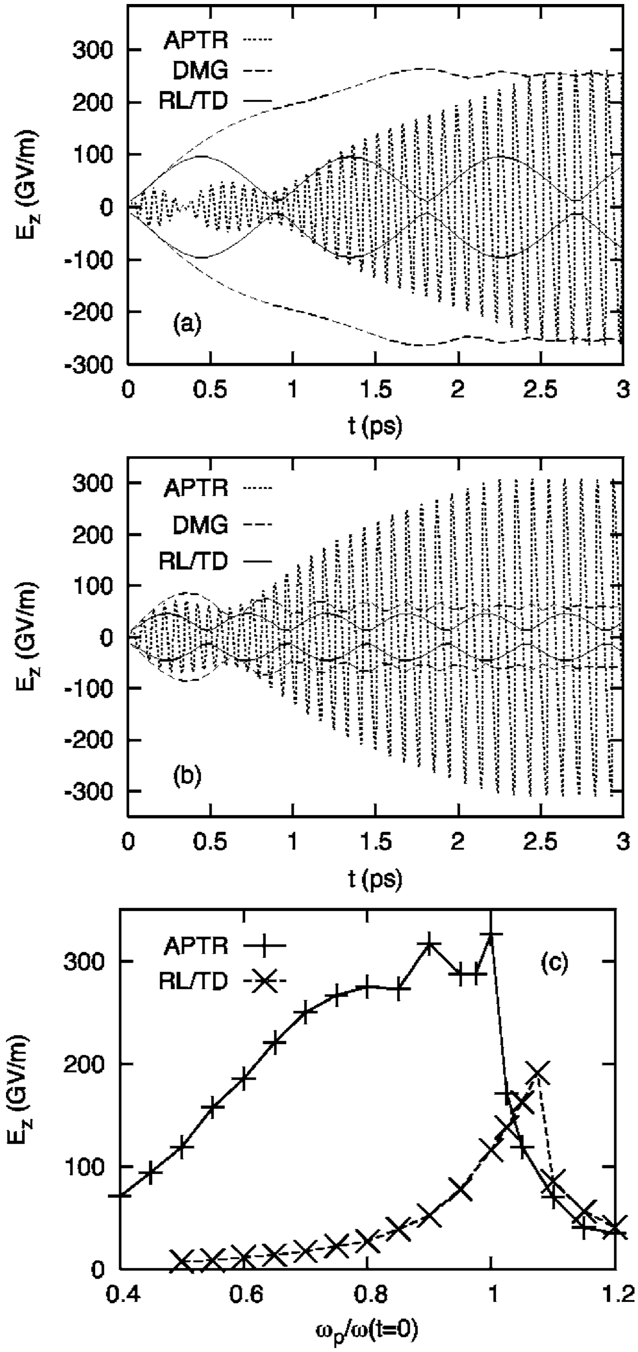

FIG. 4. Plasma wave excitation for a 800 nm Ti:sapphire laser with $\bar{\omega}/\omega_p = 25$, intensity 2×10^{17} W/cm^2 (ϵ=0.09). APTR parameters are $\Delta\omega(0) = 1.2$, and $\Delta\omega=1$ at $t\approx1.4$ ps (α=0.00225). Total chirp is 3% of the laser frequency. In (a), we see that the DMG and APTR scheme give approximately the same final fields, about three times that for on-resonance. In (b), we changed ω_p by 10%, and the excitation for the DMG and the on-resonant scheme drop considerably, while APTR maintains its large excitation. Panel (c) indicates the insensitivity of APTR to errors of ±35% in the plasma density, while still yielding large amplitude plasma waves.

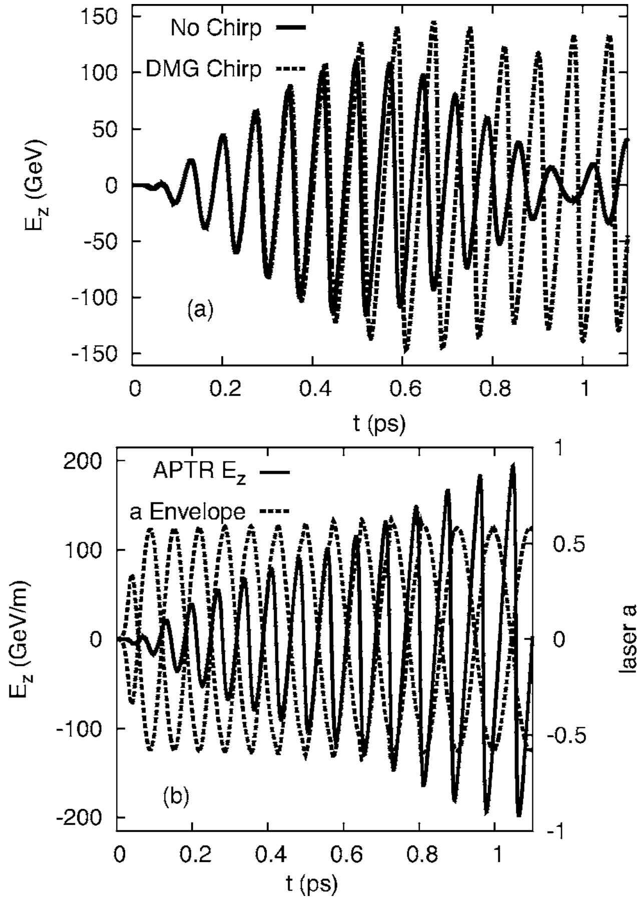

FIG. 5. Fluid simulations of the Ti:sapphire example from Sec. V B. The solid line in (a) demonstrates the RL oscillations in E_z characteristic of resonant excitation, while the dotted line indicates saturation of the DMG chirp from resonance due to failed frequency locking. The solid line in (b) shows autoresonant excitation of the plasma wave to amplitudes above E_0. The dotted line in (b) indicates some nontrivial evolution of the lasers; nevertheless, overall agreement with the simplified QSA model is quite good.

Note how the qualitative behavior of the excitation is very close to the QSA results in Figs. 4(a) and 4(b). The solid line in Fig. 5(a) demonstrates the Rosenbluth-Liu limit $E_{\mathrm{RL}}\approx125$ GV/m characteristic of resonant driving, while the DMG chirp from resonance fails to adequately phase lock the laser drive to the plasma wave, causing premature saturation. Figure 5(b), on the other hand, demonstrates large amplitude excitation to $E_z\approx200$ GV/m, above the cold, wave-breaking field of $E_0\approx160$ GV/m, but a bit less than the predicted 260 GV/m. The laser drive envelope has undergone some nontrivial evolution, but retains good frequency-locking to the plasma wave throughout the window.

VII. DISCUSSION: COMPARISONS, SCALINGS, AND PHASE LOCKING

In comparison to other PBWA schemes, including the fixed beat-frequency approach at linear resonance (RL/TD), the chirped (DMG) scheme, involving downward chirping from resonance, or the nonresonant PBWA, scheme, recently proposed by Filip *et al.*,[36,38] involving strongly forced waves at frequency shifts well below resonance in a marginally underdense plasma, the autoresonant/APTR PBWA enjoys a number of advantages, in terms of plasma wave amplitude, robustness, and quality. In previous sections we have seen how, for given drive laser intensity, autoresonant excitation yields longitudinal fields that can be considerably higher than the RL limit set by relativistic detuning of the plasma wave. We have also seen how APTR, i.e., slowly sweeping the frequency downward through resonance, provides a much greater degree of robustness to density mismatches, since neither the final amplitude nor frequency of the plasma wave is very sensitive to the precise location of the actual linear resonance.

While our simplified model has demonstrated the robustness of autoresonant excitation with respect to global density mismatches and to small changes in the laser parameters, we believe that some of this robustness should persist in the presence of moderate spatio-temporal variations and nonuniformity in either the plasma or the laser dynamics. While other excitation schemes will yield highly irregular accelerating structure in the presence of such variations, our autoresonant approach enjoys an intrinsic insensitivity and persistence, due to the local nature of the phase-locking. Provided only that the magnitude and scales for the nonuniformity are such as to allow an eikonal treatment of the waves, we expect[24] that at each position, the local plasma response will be autoresonantly excited by the drive, based on the local, slowly-varying values of the plasma frequency, drive amplitude, beat frequency, and chirp rate. Not all spatial regions will reach precisely the same final amplitude, but the wave is excited more or less everywhere until local saturation, so the final variations should be considerably less than in standard approaches. Although plausible, given what has been demonstrated in previous analyses of autoresonant phenomena, this expectation should also be verified in more realistic simulations.

The suitability of the excited plasma waves for relativistic particle acceleration depends not only on the magnitude of the peak electric fields, but even more crucially on the uniformity of the phase and phase velocity, and on the degree of phase-locking to the external drive. With variations in the group velocity $\bar{v}_g$ expected to be small [$\bar{v}_g$ varies appreciably only after propagation lengths of order the aforementioned dispersion length $L_{\rm disp} \sim (\bar{\omega}^3/\omega_p^3)(c/\omega_p)$], phase coherence of the plasma wave will depend on how closely v_p follows the essentially constant $\bar{v}_g$ of the laser. Particle-in cell (PIC) simulations of Filip *et al.*[38] suggest that for the RL/TD scheme, the effective phase velocity of the nonlinear plasma wave can vary appreciably, i.e., 10% to 20%, reflecting phase slippage of the Langmuir wave primarily as a result of relativistic detuning, while the plasma wave produced in their nonresonant PBWA scheme exhibits substantially less phase slippage. Since our autoresonant scheme also yields frequency-locked excitation, we expect to find an accelerating field of uniform phase that is everywhere directly related to the local phase of the driving beat wave.

This ostensible ability to phase-lock the plasma wave to the beat-wave of the applied drive lasers is an appealing feature of both the nonresonant PBWA and the autoresonant PBWA, since the timing of electron injection, whether based on an external cathode[39] or internal optical method,[40,41] will be provided by presumed knowledge of the laser phase. Because of its potential importance, this phase-locking deserves careful investigation. But first, one must distinguish phase-locking from frequency-locking, however much these terms are conflated. Perfect phase-locking implies perfect

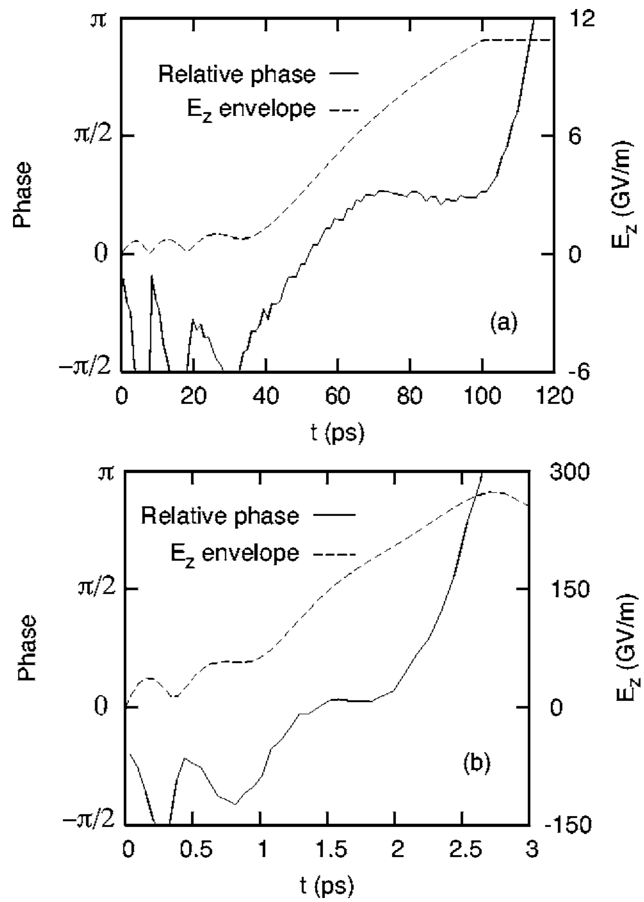

FIG. 6. Evolving phase difference between the maxima of the laser beat and the longitudinal electric field E_z (which may differ from Ψ in the text by a constant). Plot (a) uses the CO_2 laser parameters of Fig. 3, which demonstrates nearly constant phase locking throughout autoresonant excitation for $40 < t < 100$, permitting good control of electron injection. Plot (b) uses the Ti:sapphire parameters of Fig. 4 and shows tight phase-locking during the beginning of excitation $t < 2$ ps, at which time $E_z \approx 225$ GV/m.

frequency-locking, and conversely, (at least up to a constant phase), but in the case of imperfect entrainment, it is possible to achieve good frequency-locking without adequate phase-locking, or the converse. Whether the relative error in phase-matching or in frequency-matching between driving and driven oscillation is greater depends on whether the Fourier content of fluctuations in the phase is primarily at higher or lower frequencies than the drive frequency itself.

For the purpose of matched particle injection, it is phase-locking that is desired, yet some caution is warranted in claims of true phase-locking in either the nonresonant or autoresonant PBWA. In any frequency-locked PBWA scheme, the nonlinear frequency of the Langmuir wave may be closely entrained to the precisely known drive frequency, but this does not necessarily imply that the absolute phase of the Langmuir wave may be precisely known. As a mechanism for phase-locking in the nonresonant PBWA, the authors appeal to the claim that an harmonic oscillator, strongly driven off resonance, remains synchronous with the driving force. However, this intuition holds only for damped linear oscillators after the transient is allowed to decay. If a linear oscillator with natural frequency ω_n is forced by a sinusoidal drive with frequency $\omega_d < \omega_n$, then, independent of the strength of the drive, the driven oscillator will exhibit persistent, oscillating variations in phase relative to the drive phase $\psi_d = \omega_d t + \psi_d(0)$, which are $\sim O(\omega_d/\omega_n)$; i.e., only first order in their frequency ratio. There is no obvious reason to expect in general that nonlinearities will improve matters.

In the autoresonant case, we encounter good frequency-locking with comparably good phase locking only over some portion of the Langmuir excitation, depending on the drive parameters. In Fig. 6 we plot, for our experimentally motivated parameters of Sec. V, the phase lag between the beat-wave of the lasers and the plasma wave, numerically estimated by the offset between corresponding relative maxima. In the case of the CO_2 laser parameters, Fig. 6(a) indicates that once the laser beat passes through the linear resonance, the plasma wave phase tightly locks with the drive phase and remains so until adiabaticity is lost and the excitation saturates. In this case, a phase-locked injection scheme could reliably place electron bunches near the maximum acceleration gradient ~11 GV/m.

While the Ti:sapphire example in Fig. 6(b) also initially experiences tight phase-locking to the drive, we see that the phase difference between the laser beat and the Langmuir wave drifts during the latter stages of excitation, eventually reaching π at saturation. Thus, the highest-amplitude fields during the final stages of excitation experience some phase slippage from the lasers, and one may not be able to reliably inject particles into the largest accelerating gradients achieved. Nevertheless, the longitudinal field reaches an amplitude of approximately 225 GV/m while the phase is tightly locked, thus permitting controlled, phase-locked injection into accelerating fields above both $E_{RL} \approx 125$ GV/m and $E_0 \approx 200$ GV/m.

VIII. CONCLUSION

We have introduced a straightforward, seemingly minor, modification of the DMG scheme for the chirped-pulse PBWA, based on the nonlinear phenomenon of autoresonance with adiabatic passage through resonance, which nevertheless enjoys certain advantages over previous approaches. Rather than starting at the linear resonance and chirping downward using a profile expected to match the decreasing nonlinear plasma frequency, we start above resonance and sweep the beat frequency downward through the resonance, at any sufficiently slow chirp rate, such that the plasma wave frequency automatically self-locks to the drive frequency, and the plasma wave amplitude automatically adjusts itself consistent with this frequency. This autoresonant excitation achieves higher plasma wave amplitudes at moderate laser intensities, and, most importantly, appears to be much more robust to inevitable uncertainties and variations in plasma and laser parameters. Preliminary analysis has been performed within a simplified analytic and numerical model, and wake excitation has been studied using realistic parameters for Ti:sapphire and CO_2 laser systems. The results have been substantiated with self-consistent 1D fluid simulations, and warrant extending investigation to higher-dimensional geometries and more realistic plasma inhomogeneities via numerical solution with additional fluid and PIC codes.

ACKNOWLEDGMENTS

This research was supported by the Division of High Energy Physics, U.S. Department of Energy, Grant Number DE-FG02-04ER41289, and by the US–Israel Binational Science Foundation (Grant No. 2004033).

[1] J. Tajima and J. Dawson, Phys. Rev. Lett. **43**, 267 (1979).
[2] N. Kroll, A. Ron, and N. Rostoker, Phys. Rev. Lett. **13**, 83 (1964).
[3] B. Cohen, A. Kaufman, and K. Watson, Phys. Rev. Lett. **29**, 581 (1972).
[4] M. Rosenbluth and C. Liu, Phys. Rev. Lett. **29**, 701 (1972).
[5] C. Joshi, W. Mori, T. Katsouleas, J. Dawson, J. Kindel, and D. Forslund, Nature **311**, 525 (1984).
[6] B. Amini and F. Chen, Phys. Rev. Lett. **53**, 1441 (1984).
[7] C. Tang, P. Sprangle, and R. Sudan, Phys. Fluids **28**, 1974 (1985).
[8] C. Clayton, C. Joshi, C. Darrow, and D. Umstadter, Phys. Rev. Lett. **54**, 2343 (1985).
[9] R. Noble, Phys. Rev. A **32**, 460 (1985).
[10] W. Mori, IEEE Trans. Plasma Sci. **PS-15**, 88 (1987).
[11] P. Mora, D. Pesme, A. Héron, G. Laval, and N. Silvestre, Phys. Rev. Lett. **61**, 1611 (1988).
[12] Y. Kitigawa, T. Matsumoto, T. Minamihata *et al.*, Phys. Rev. Lett. **68**, 48 (1992).
[13] M. Everett, A. Lal, D. Gordon, C. Clayton, K. Marsh, and C. Joshi, Nature **368**, 527 (1994).
[14] C. Clayton, C. Joshi, K. Marsh, C. Pellegrini, and J. Rosenzweig, Nucl. Instrum. Methods Phys. Res. A **410**, 378 (1998).
[15] E. Esarey, P. Sprangle, J. Krall, and A. Ting, IEEE Trans. Plasma Sci. **24**, 252 (1996).
[16] A. Akhiezer and R. Polovin, Sov. Phys. JETP **3**, 696 (1956).
[17] J. Dawson, Phys. Rev. **113**, 383 (1959).
[18] C. McKinstrie and D. Forslund, Phys. Fluids **30**, 904 (1987).
[19] G. Shvets, Phys. Rev. Lett. **93**, 195004 (2004).
[20] J. Matte, F. Martin, N. Ebrahim, P. Brodeur, and H. Pepin, IEEE Trans. Plasma Sci. **PS-15**, 173 (1987).
[21] M. Deutsch, B. Meerson, and J. Golub, Phys. Fluids B **3**, 1773 (1991).
[22] A. Loeb and L. Friedland, Phys. Rev. A **33**, 1828 (1986).
[23] B. Meerson and L. Friedland, Phys. Rev. A **41**, 5233 (1990).
[24] L. Friedland, Phys. Fluids B **4**, 3199 (1992).
[25] L. Friedland, Phys. Rev. E **58**, 3865 (1998).
[26] P. Sprangle, E. Esarey, and A. Ting, Phys. Rev. Lett. **64**, 2011 (1990).
[27] D. Forslund, J. Kindel, and E. Lindman, Phys. Rev. Lett. **30**, 739 (1973).
[28] C. Max, J. Arons, and A. Langdon, Phys. Rev. Lett. **33**, 209 (1974).
[29] P. Sprangle, E. Esarey, and A. Ting, Phys. Rev. Lett. **64**, 2011 (1991).
[30] *Table of Integrals, Series, and Products*, edited by I. Gradshteyn and I. Ryzhik (Academic, New York, 1980).
[31] B. Chirikov, Phys. Rep. **52**, 263 (1979).
[32] F. Lewis, Trans. ASME **54**, 253 (1932).
[33] E. Grosfeld and L. Friedland, Phys. Rev. E **65**, 046230 (2002).
[34] J. Fajans, E. Gilson, and L. Friedland, Phys. Plasmas **6**, 4497 (1999).
[35] D. Strickland and G. Mourou, J. Opt. Commun. **56**, 219 (1988).
[36] C. Filip, S. Tochitsky, R. Narang, C. Clayton, K. Marsh, and C. Joshi, AIP Conf. Proc. **647**, 770 (2002).
[37] B. Shadwick, G. Tarkenton, E. Esarey, and W. Leemans, IEEE Trans. Plasma Sci. **30**, 38 (2002).
[38] C. Filip, R. Narang, S. Tochitsky, C. Clayton, P. Musumeci, R. Yoder, K. Marsh, J. Rosenzweig, C. Pellegrini, and C. Joshi, Phys. Rev. E **69**, 026404 (2004).
[39] C. Clayton and L. Serafini, IEEE Trans. Plasma Sci. **24**, 400 (1996).
[40] E. Esarey, R. Hubbard, W. Leemans, A. Ting, and P. Sprangle, Phys. Rev. Lett. **79**, 2682 (1997).
[41] C. Schroeder, P. Lee, J. Wurtele, E. Esarey, and W. Leemans, Phys. Rev. E **59**, 6037 (1999).